

Article

Chitosan Hydrogels Crosslinked by Genipin and Reinforced with Cellulose Nanocrystals: Production and Characterization

Andréia Aparecida do Nascimento Pomari ¹, Thaís Larissa do Amaral Montanheiro ^{2,*} ,
Cristiane Pereira de Siqueira ¹, Rodrigo Sousa Silva ¹, Dayane Batista Tada ³ and
Ana Paula Lemes ^{1,*}

¹ Laboratory of Polymers and Biopolymers, Institute of Science and Technology, Federal University of São Paulo (UNIFESP), Talim, 330–São José dos Campos, SP 12.231-280, Brazil

² Laboratory of Plasmas and Processes, Technological Institute of Aeronautics, Praça Marechal Eduardo Gomes, 50-Vila das Acácias, São José dos Campos, SP 12228-900, Brazil

³ Laboratory of Nanomaterials and Nanotoxicology, Institute of Science and Technology, Federal University of São Paulo (UNIFESP), Talim, 330–São José dos Campos, SP 12.231-280, Brazil

* Correspondence: tlamontanheiro@gmail.com (T.L.d.A.M.); aplemess@gmail.com (A.P.L.);
Tel.: +55-12-99192-2199 (T.L.d.A.M.); +55-12-98133-9889 (A.P.L.)

Received: 28 June 2019; Accepted: 6 August 2019; Published: 13 August 2019



Abstract: In this work, chitosan hydrogels crosslinked with genipin and reinforced with cellulose nanocrystals (CNC) were developed and characterized with the aim of future biomedical applications. CNC was produced by acid hydrolysis and characterized by atomic force microscopy (AFM). Chitosan/CNC nanocomposite hydrogels were produced with different CNC concentrations (*w/w*): 0%, 2%, 4%, and 6%. The genipin was used as a crosslinking agent in a genipin/chitosan molar proportion of 1:8. The hydrogels were characterized by porosity measurements, scanning electron microscopy (SEM), swelling test, and mechanical compression test. No significant differences were observed concerning the porosity of the hydrogels; however, a trend of decreasing porosity was observed with increasing CNC content. The SEM images showed a better pore structure as the CNC concentration increased. A decrease in the swelling degree with increasing CNC content in the chitosan/CNC nanocomposite hydrogel was verified in the swelling tests. An increase in the CNC concentration in the chitosan/CNC nanocomposite hydrogel caused a gradual increase in the maximum stress and maximum strain as observed in the compression tests, showing a significant difference between chitosan/CNC 6 wt % and neat chitosan hydrogel.

Keywords: hydrogel; chitosan; cellulose nanocrystal; genipin

1. Introduction

The development of new biomaterials has been an essential tool to improve the treatment of various diseases, traumas, and other medical problems of several complexity degrees. Advances in materials science, in both their production and their characterization techniques, have driven the development of biomaterials which present increasingly specific properties according to their application [1,2].

Among the different types of biomaterials, hydrogels have been one of the most used, since the versatility of their physical properties and their capacity for water absorption make them suitable for use for different purposes [3], such as the production of contact lenses, artificial cartilage, controlled drug delivery systems, dressings, and implants and filling material for aesthetic and reconstruction purposes, among others [4–6].

Hydrogels may be produced from synthetic polymers such as polyacrylamide (PAM) [7] or natural polymers, such as chitosan, among others [8–11]. The great advantage in the use of natural polymers is the ability to interact with cells and cellular enzymes and to be remodeled and/or degraded to provide a place for tissue growth [12]. Thus, these hydrogels can provide the appropriate support for cell proliferation and, at the same time, provide the necessary mechanical resistance to maintain the new tissue.

Chitosan presents several interesting properties for the production of hydrogels for medical applications, such as biocompatibility, biodegradability, non-toxicity, antimicrobial activity, and the ability to accelerate the healing process [13]. The production of chitosan hydrogels, like other polymers, involves the formation of crosslinks between the polymer chains in order to obtain the three-dimensional polymer network (crosslinking) [11]. Thus, the choice of crosslinking agent is very important since its chemical structure can influence the characteristics of the hydrogel.

Among the possible crosslinking agents, genipin has been widely studied due to its natural origin, low cytotoxicity, and great biocompatibility compared to other conventional crosslinkers [14]. It presents in its chemical structure two reactive sites through which occur its connection with a polymer matrix, forming the three-dimensional polymer network.

However, the low mechanical properties of chitosan hydrogel crosslinked with genipin hamper its application in cases where it is subjected to stress such as traction, compression, shear, and torsion. For this reason, the introduction of reinforcing nanofillers into chitosan matrixes has been evaluated both in the production of engineering materials and in the production of biomaterials [5,6,15].

One of the most studied nanofillers is cellulose nanocrystals (CNC) since their nanometric dimensions result in increased mechanical resistance when used in low concentrations in the final material. In addition, the renewable origin, non-toxicity, and hydrophilicity of CNC make them a potential candidate for the reinforcement of biomaterials [1,16].

The introduction of CNC in different chitosan matrixes has been extensively studied, and several improvements in its properties have been verified, including increased tensile strength, thermal stability, and water resistance, along with decreased permeation to water vapor and swelling degree [5,17–22].

However, most of these works have reported on the production of chitosan films and membranes with CNC, and these materials were mainly evaluated by tensile tests. Besides that, to the best of our knowledge, there have been no reports about chitosan hydrogels reinforced with CNC using genipin as a crosslinking agent in the literature. Therefore, this work reports not only on an original formulation but also on a new target application. Whereas a film could only be useful as a coating, the hydrogel would be useful in various biomedical applications such as in grafting, dressing, and scaffolding for tissue engineering. Therefore, in this work, the effect of CNC introduction on chitosan hydrogels crosslinked with genipin was evaluated, aiming towards the development of a biocompatible, biodegradable, and low-toxicity material with satisfactory mechanical properties for future biomedical applications.

2. Materials and Methods

Chitosan from Sigma-Aldrich (St. Louis, MO, USA) with 75–85% deacetylation and classified as medium molecular mass was used to produce the hydrogels. Genipin, used as the crosslinking agent, was produced by CBC-Challenge Bioproducts CO (Yun-Lin Hsien, Taiwan) with 98% purity and with a molar mass of $226.2 \text{ g}\cdot\text{mol}^{-1}$. Glacial acetic acid from Merck (Darmstadt, Germany) was used to solubilize the chitosan.

The cellulose nanocrystals (CNC) used in this work were produced from the acid hydrolysis of cellulose microcrystals (Sigma-Aldrich, $\sim 20 \mu\text{m}$, $d = 0.6 \text{ g}\cdot\text{cm}^{-3}$) using sulfuric acid (analytical grade) from Neon Comercial (Sao Paulo, Brazil).

For the production of the CNC suspension, microcrystalline cellulose was added into a flask containing a 64% (*w/w*) aqueous solution of sulfuric acid. The suspension was mixed for 90 min at $45 \text{ }^\circ\text{C}$. To stop the hydrolysis process, the suspension was placed in an ice bath and distilled water was added to the mixture. The suspension was centrifuged and washed with distilled water and placed on dialysis

for 2 days to obtain neutral pH. Finally, it was sonicated for 5 min in an ultrasonic processor ((VCX 750, Sonics & Materials, Inc., Newtown, CT, USA), 750 W and 20 kHz).

To determine the CNC concentration in the suspension, three samples of 1 mL were collected and placed in different plastic tubes. Each sample was frozen and lyophilized. The CNC dry mass in each tube was weighed and the average mass calculated. CNC dimensions were determined by atomic force microscopy (AFM). Samples were previously dispersed in water, dripped in cleaved mica, and dried with nitrogen flux. Images were obtained in a Nanoscope V (Veeco Instruments, Inc., Santa Barbra, CA, USA) using the non-contact mode.

Hydrogel samples were produced with the addition of 25 mg of chitosan to 2 mL of 1% (v/v) acetic acid aqueous solution. The mixture was stirred and then placed in an ultrasonic bath for 5 min at room temperature. To start the crosslinking reaction, 1 mL of genipin aqueous solution ($4.4 \text{ mg}\cdot\text{mL}^{-1}$) in 1% (v/v) acetic acid aqueous solution was added to the chitosan solution in order to obtain a molar ratio of 1:8 (genipin/chitosan). The genipin solution was previously prepared and sonicated for 5 min.

After the addition of genipin, the resulting solution was stirred for 1 min at room temperature and then poured into a plastic tube. The tubes were kept at room temperature for 7 days to produce cylindrical chitosan hydrogels. The same was done to produce chitosan/CNC hydrogels; however, before the addition of genipin, the CNC stock suspension, previously prepared as described previously, was added to the chitosan solution in order to obtain hydrogels with 2%, 4%, and 6% ($W_{\text{CNC}}/W_{\text{chitosan}}$) and stirred for 10 min. The crosslinking reaction between chitosan and genipin with molecular structures is shown in Figure 1.

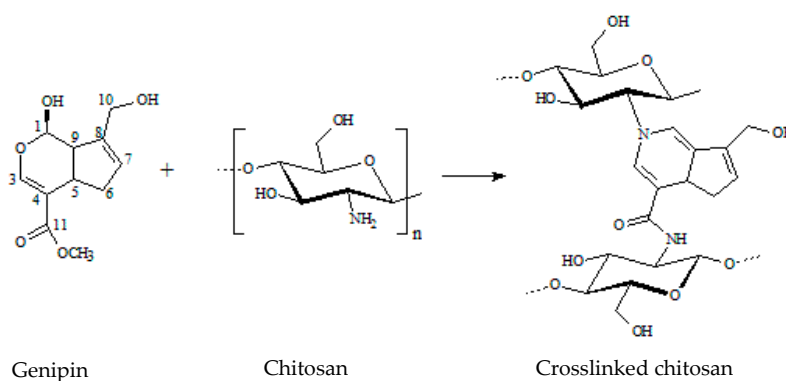


Figure 1. Crosslinking reaction between chitosan and genipin.

The hydrogel's porosity was determined using the liquid displacement method [23,24]. Three samples of each hydrogel group with known weight (W_1) were immersed in ethanol for a duration of 24 h. The wet weight was recorded (W_2), and the porosity was calculated using Equation (1):

$$P (\%) = \frac{W_2 - W_1}{V_s \times \rho_e} \quad (1)$$

where W_1 is the dry weight of the hydrogel, W_2 is the wet weight, V_s is the hydrogel volume (measured with a caliper rule), and ρ_e is ethanol's density.

The cryogenic fracture surface of the chitosan/CNC hydrogels produced with different CNC concentrations (0%, 2%, 4%, and 6% ($W_{\text{CNC}}/W_{\text{chitosan}}$)) was analyzed in a JEOL JSM-T300 SEM (JEOL Ltd., Peabody, MA, USA) with secondary electron detectors to evaluate their internal morphology. For this test, the swollen samples were lyophilized, fractured in liquid N_2 , supported on a stub, and sputter-coated with gold.

To perform the swelling test, five samples from each hydrogel group were weighed and then immersed in distilled water at 37°C and neutral pH. At intervals of 30 min, the samples were removed from the water, dried rapidly with a paper towel to remove excess water, and then weighed on

an analytical balance. This process was repeated until each sample had a constant weight, and the swelling degree was obtained according to Equation (2):

$$S(\%) = \frac{W_1 - W_0}{W_0} \times 100 \quad (2)$$

where W_0 is the initial weight of the sample after production in the cylindrical mold and W_1 is the weight of the swollen sample.

Compressive mechanical tests were performed with five samples from each hydrogel group with dimensions of 1 cm diameter and 2 cm length in a Brookfield CT3 Texturometer (AMETEK Brookfield, Middleboro, MA, USA), with a probe of 25.4 mm diameter and 35 mm length, a 50 kg load cell, and 0.2 mm/s test speed. The test determined the maximum stress (kPa) and the maximum compression strain.

All data are expressed as mean \pm SD and were analyzed using analysis of variance (ANOVA) and Tukey–Kramer testing. $p < 0.05$ was considered significant.

3. Results and Discussion

3.1. Characterization of CNC Suspension

Figure 2 shows the AFM images of the produced CNC. It was possible to observe the elongated and thin needle form typical of CNC [1,16]. The mean length and mean diameter values were calculated by analyzing the obtained images. In addition, using the values of length and diameter, the aspect ratio of CNC was calculated.

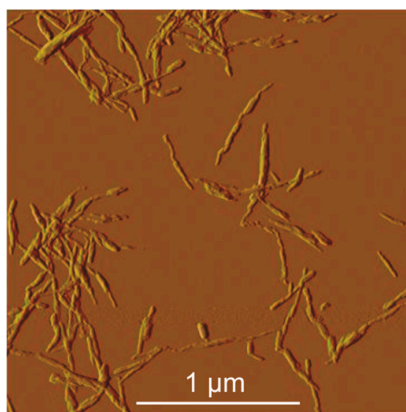


Figure 2. Atomic force microscopy (AFM) depth image of cellulose nanocrystals (CNC) (2.5 μm \times 2.5 μm).

The lengths ranged from 150 to 350 nm with a mean value of 250 nm, while the diameter was in the range of 15–35 nm with a mean value of 25 nm. These values are comparable to those obtained by Shaheen et al. [25], who reported lengths and diameters ranging from 140 to 423 nm and 21 to 47 nm, respectively. Besides that, the results are also similar to the results obtained with CNC produced by other processes, such as acid hydrolysis with oxalic acid solution, through which Song et al. [26] obtained CNC with the same needle-like morphology with length and diameter around 300 nm and 10 nm, respectively. By using phosphoric acid solution, Wang et al. [27] obtained CNC with lengths ranging from 100 to 330 nm and diameter ranging from 2 to 6 nm.

The mean value of the aspect ratio was 10, and as described by the literature [28,29], this is the minimum value required to obtain satisfactory stress transfer from the matrix to the fibers.

The concentration of CNC in the suspension was obtained to determine the volume that would be necessary to produce chitosan/CNC hydrogels with 0, 2, 4, and 6 wt % of CNC. An average value of (23 \pm 2) $\text{mg}\cdot\text{mL}^{-1}$ was obtained from the lyophilized weight values of three aliquots of 1 mL taken from the original suspension.

3.2. Chitosan Crosslinking by Genipin

During the crosslinking reaction, the appearance of blue color was observed from the surface to the bottom of the hydrogels (Figure 3A). After 7 days, the hydrogel presented a homogeneous blue color throughout its length, regardless of the presence or absence of CNC (Figure 3B,C). This time was necessary due to the small contact surface of the hydrogel with the atmosphere, which restricted its contact with O₂. This observation is in agreement with results by Pujana and co-workers [30], where the crosslinking reaction of chitosan by genipin was also complete after 7 days. The blue coloration is explained by the oxygen radical-induced polymerization of genipin and the dehydrogenation of intermediate compounds [31,32].

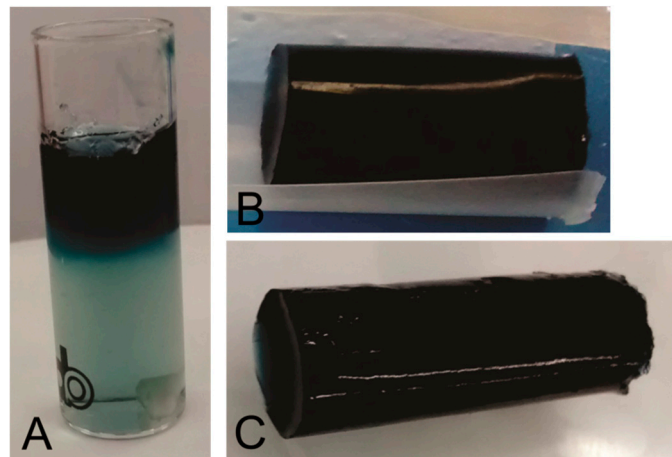


Figure 3. (A) Evolution of the crosslinking process of chitosan with genipin accompanied by the appearance of blue coloration; (B) chitosan hydrogel after 7 days of crosslinking with genipin, and (C) chitosan hydrogel with 6% CNC after 7 days of crosslinking with genipin.

3.3. Porosity

The porosity of hydrogels is commonly modified by the presence of nanoparticles in the polymeric matrix. Also, porosity defines other properties of hydrogels such as the swelling degree and mechanical resistance. Therefore, the porosity was measured herein in order to understand the influence of CNC concentration on this property. According to Equation (1), the mean porosity value for each CNC percentage was calculated by using the difference between the dry and wet weight and is presented in Figure 4.

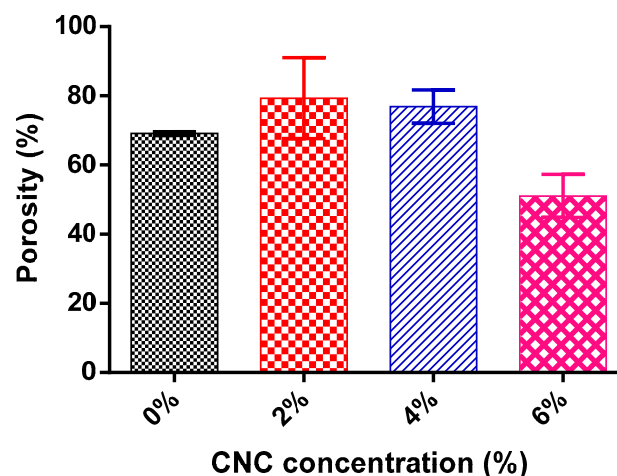


Figure 4. Porosity values obtained by the liquid displacement method of dry samples of chitosan/CNC hydrogels.

The porosity values of hydrogels with 0, 2, and 4 wt % CNC were about 69, 79, and 77, respectively. These values are similar to those reported for chitosan hydrogels with different crosslinkers and for hydrogels resulting from a combination of chitosan with other polymers [8,33–35]. For example, Carvalho and Mansur [35] reported porosity values of 69% to 88% for methacrylamide–chitosan hydrogels. Nevertheless, the porosity of the hydrogel containing 6% of CNC was 51%, a value significantly lower than those of the other samples or reported in the literature. Thus, although no statistical difference was observed for this value compared to the others, a tendency of decreasing porosity is observed with increasing CNC content. It is well known that the addition of nanofillers to a hydrogel may decrease the porosity [1,8,33]. Montanheiro et al. [1] reported a decrease of ~20% in the poly(hydroxybutyrate-co-hydroxyvalerate) (PHBV) scaffolds porosity due to the addition of 3% (wt %) of CNC. Ferreira et al. [8] showed a decrease in chitosan hydrogel porosity from 88% to 82.4% upon the addition of 6% (wt %) of CNC. Herein, a similar ratio of chitosan to CNC resulted in a more significant decrease of porosity. Most probably, in the presence of CNC, ionic crosslinking took place between the negatively charged CNC [16] and the positively charged chitosan since the mixture was in an acidic medium. Therefore, the simultaneous crosslinking processes, one from the reaction between genipin and chitosan and the other from the ionic interaction with CNC, resulted in the lower porosity. In the work of Ferreira et al. [8], the effect of CNC addition was less drastic since the chitosan hydrogel analyzed by them was obtained through crosslinking reaction with glutaraldehyde, which is known to be a more efficient crosslinker than genipin. Therefore, in their samples, there was lower availability of protonated amino groups of chitosan to interact with CNC.

3.4. Scanning Electron Microscopy

Figure 5 shows SEM images from the fracture surface of chitosan/CNC hydrogels produced with 0, 2, 4, and 6 wt % of CNC. With the addition of CNC, the structure became more compact, in the form of layered leaves. This may have been due to a collapse of the sample during the drying process, which did not happen for hydrogels with CNC due to structural reinforcement caused by the filler of 4% CNC. The concentration of 2% CNC was not enough to promote this structural reinforcement. For this reason, a better pore structure with increasing CNC concentration was observed. However, it was not possible to detect significant differences regarding the porosity or even the roughness of the internal pore walls of chitosan hydrogels produced with different CNC concentrations.

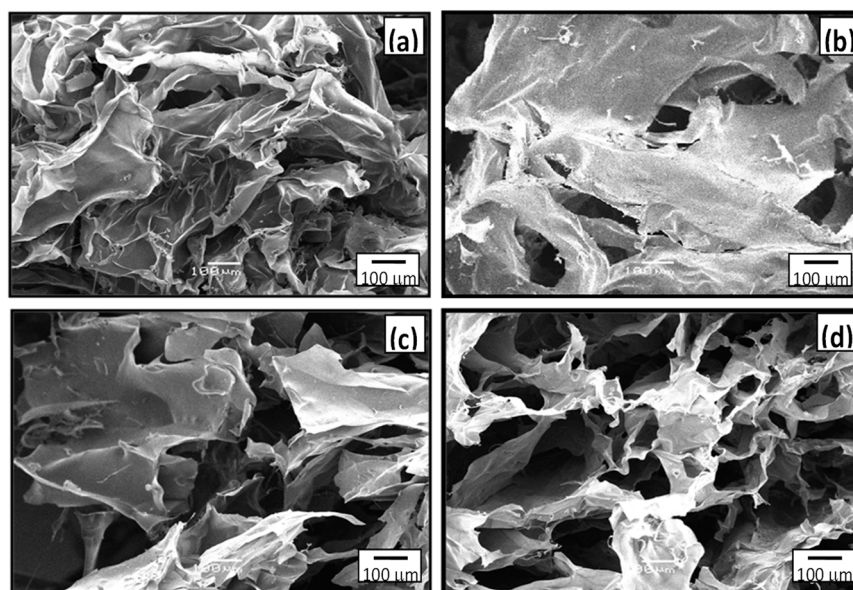


Figure 5. Scanning electron microscopy (SEM) images with 100× magnification of hydrogels (a) chitosan (b) chitosan/CNC 2% (c) chitosan/CNC 4%, and (d) chitosan/CNC 6%.

Naseri et al. [36] produced scaffolds of cellulose nanofibers and a genipin-crosslinked matrix of gelatin and chitosan. The authors reported flat and layered hydrogel morphologies for samples with a higher content of the matrix, corroborating the behavior reported in this work.

3.5. Swelling Tests

Figure 6 shows the swelling kinetics of hydrogels as the mean of five samples. Statistical analysis was done comparing the chitosan/CNC hydrogels with chitosan hydrogel.

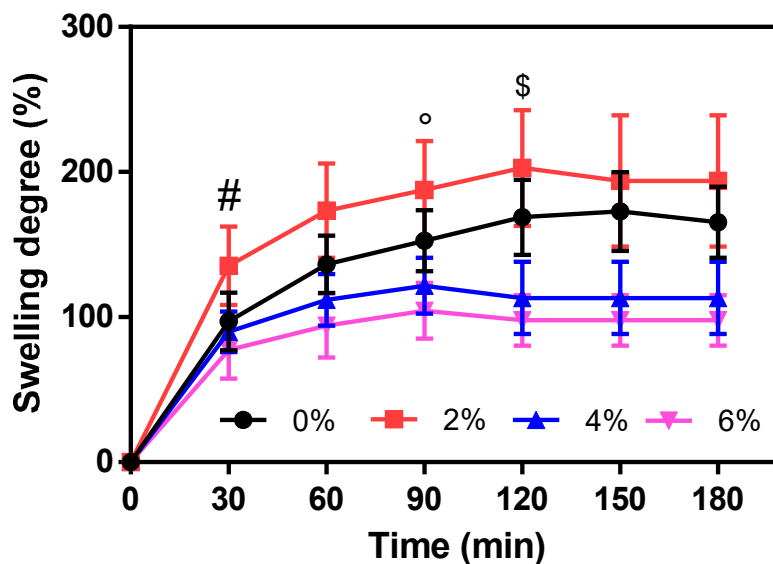


Figure 6. Swelling kinetics of chitosan/CNC hydrogels. Results are given as mean \pm SD ($n = 5$). One-way ANOVA, significance level: # $p < 0.05$ between 0% CNC and 2% CNC; ° $p < 0.05$ between 0% CNC and 6% CNC; \$ $p < 0.05$ between 0% CNC and 4% CNC; and $p < 0.01$ between 0% CNC and 6% CNC (statistical differences shown for groups compared to 0% CNC).

Regarding the swelling kinetics, all samples followed the same pattern, with a high swelling rate in the first 30 min and a gradual decrease of the swelling rate until reaching the maximum swelling degree. It was observed that the hydrogel without CNC took the longest time to reach the maximum swelling degree—about 180 min. This time decreased with increasing CNC content in the hydrogel. Chitosan/CNC hydrogel with 2 wt % CNC presented the maximum swelling degree after 150 min. Both hydrogels with 4 and 6 wt % required 120 min to complete the swelling process. As the addition of CNC restricts hydrogel deformation by making its walls more rigid, the water absorption capacity decreases. Thus, as the total amount of absorbed water was lower, the maximum swelling was reached in a shorter time. However, the slopes of the swelling curves show that for higher CNC concentrations (4% and 6%) the absorption rate was lower compared to pure or 2% CNC chitosan hydrogel.

A comparison between the hydrogels' maximum swelling degrees is important to verify the influence of CNC on the total water absorption capacity (Figure 7) since the maximum swelling degree was achieved at different times for each kind of hydrogel. The maximum swelling degree was displayed by the 2% CNC hydrogel. However, further increasing CNC concentration (4% and 6%) promoted a sharp decrease in the maximum swelling degree. The maximum swelling degrees of the hydrogels with 0, 2, 4, and 6 wt % CNC, obtained at the maximum swelling time, were about 165%, 194%, 113%, and 98%, respectively. In the hydrogel with 2% of CNC, the diffusion of water into the hydrogel may be promoted by the high hydrophilicity of CNC [16], and the increase in the rigidity was not enough to prevent the hydrogel swelling. For the samples with 4 and 6 wt % of CNC, the restriction in deformation was more pronounced than the influence of the hydrophilicity of CNC, and for this reason, these samples presented smaller swelling degrees. This agrees with the results observed by SEM, in which it was verified that the concentration of 2% CNC did not promote

the structural reinforcement required to prevent hydrogel wall collapse in the drying process. Thus, no significant difference was observed between chitosan/CNC 2% hydrogel and chitosan hydrogel or between chitosan/CNC 4% and chitosan/CNC 6%. In this last case, despite the structural reinforcement caused by the higher concentration of CNC (6%), the high CNC hydrophilicity may have occasioned greater diffusion of water into the hydrogel, attenuating the effect of decreasing the swelling degree. Significant differences were observed between chitosan and chitosan/CNC 4% ($p \leq 0.05$), chitosan and chitosan/CNC 6% ($p \leq 0.01$), chitosan/CNC 2% and chitosan/CNC 4% ($p \leq 0.01$), and chitosan/CNC 2% and chitosan/CNC 6% ($p \leq 0.001$).

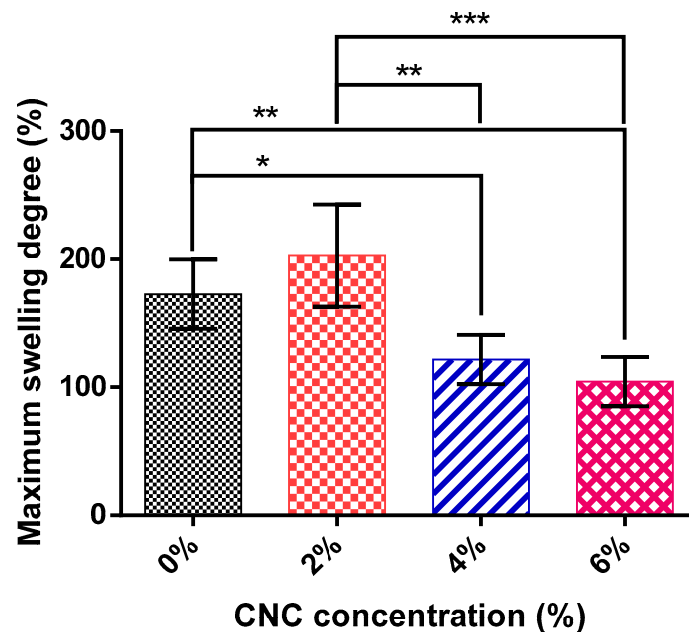


Figure 7. Maximum swelling degree of chitosan/CNC hydrogels. Results are given as mean \pm SD ($n = 5$). One-way ANOVA, significance levels: * $p \leq 0.05$, ** $p < 0.01$, *** $p < 0.001$.

The hydrogel porosity also influences the swelling degree and kinetics in a directly proportional way; thus, higher porosities result in higher swelling degrees. Although there was no significant difference between the hydrogels' porosity values, a decrease in the porosity of the hydrogels was observed with increasing CNC content, which agrees with the decrease of the swelling degree observed.

3.6. Compression Mechanical Test

Hydrogel samples with dimensions around 1 cm in diameter and 2 cm in height were subjected to mechanical compression tests to verify the effects of CNC addition on the stress and strain properties. The tests were performed following the scheme shown in Figure 8, and the results of maximum stress and maximum strain obtained in the mechanical compression test are shown in Figure 9.

The maximum stress versus CNC concentration graph is shown in Figure 9A, and the maximum strain versus CNC concentration is shown in Figure 9B. An increase in both maximum stress and maximum strain as a function of the CNC concentration in the hydrogel was observed. An increase of about 36% was obtained for the sample produced with 6 wt % of CNC compared to neat chitosan hydrogel. Similar effects were observed in another study [37] in which the addition of nanofibrillar cellulose to chitosan films caused a significant increase in its mechanical properties. Montanheiro et al. [1] reported an increase of about 63% in the compression modulus of PHBV scaffolds reinforced with 3 wt % of CNC.

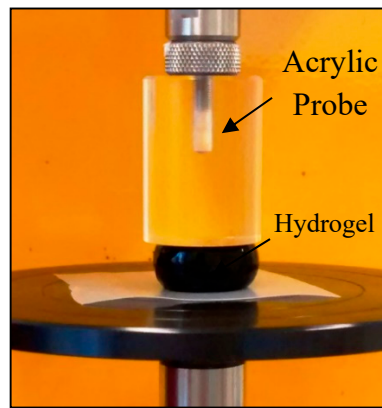


Figure 8. Representative compression test of neat chitosan hydrogel.

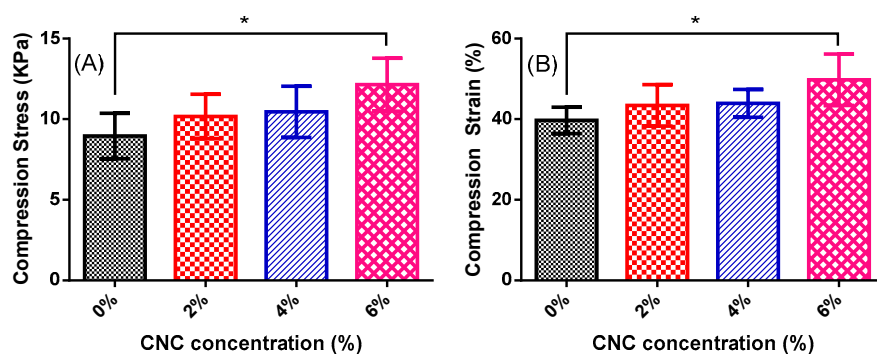


Figure 9. (A) Maximum stress × CNC concentration and (B) maximum strain × CNC concentration. Results are given as mean \pm SD ($n = 5$). One-way ANOVA, significance level: * $p \leq 0.05$.

A single-factor ANOVA test with 95% confidence was used to determine statistical differences between groups. A two-sample t -test was also used to evaluate the results. p -values less than 0.05 were considered to be statistically significant.

The gradual increase of the maximum stress and maximum strain as function of CNC concentration led to a statistically significant difference for the sample containing 6% CNC when compared to that produced with neat chitosan ($p = 0.0317$ for maximum stress and $p = 0.0297$ for maximum strain); however, there was no statistically significant difference between the hydrogels with 0%, 2%, and 4% CNC. Therefore, CNC effectively acts as a reinforcing agent for concentrations from 6% due to the effect of the hard phase (CNC) into the softer chitosan matrix [38]. Notably, the enhanced crosslinking due to ionic interaction between chitosan and CNC must also be taken into account to explain the effect of CNC on the mechanical properties of chitosan hydrogel. According to the molecular structure of chitosan and CNC, it may be assumed that the polymeric filler and matrix present strong intermolecular interactions, which contributes to effective surface adhesion between the nanofiller and polymeric matrix, resulting in better mechanical properties. Chitosan and cellulose polymers are polysaccharides [21], which present a large number of hydroxyl functional groups. Therefore, strong intermolecular hydrogen bond interaction can be established between the chains of these polymers. Besides this, CNC and chitosan chains have an ionic attraction. This is because the CNC used in this work has a negative surface charge due to the presence of ($-\text{SO}_4^-$) groups from the production process by acid hydrolysis with H_2SO_4 , while chitosan presents the protonated amine functional groups ($-\text{NH}_3^+$) due to its solubilization in acid medium with low pH. The enhanced mechanical compressive properties of the 6 wt % CNC hydrogel may also be due to the reduced porosity of this sample, as it is known that the porosity directly affects the mechanical properties of porous structures [1,39,40].

4. Conclusions

The crosslinking of chitosan hydrogel by genipin was able to be visually monitored through the bluish coloration that was more intense along the samples. CNC provided greater stiffness to the hydrogel structure, which decreased the swelling degree. Thus, hydrogels containing higher concentrations of CNC showed less capacity to swell and their structures ruptured before the others with lower CNC contents, evidencing the influence of CNC on the hydrogel structure. The compressive mechanical properties were improved with the addition of CNC. Therefore, the addition of CNC is an alternative to produce chitosan hydrogels with low genipin concentrations, since CNC increases the hydrogel resistance without the need for further addition of the crosslinker reactant. Therefore, the use of CNC as a reinforcing agent is very promising in chitosan hydrogels because it is easy to produce, non-toxic, and comes from renewable raw material found in abundance in nature.

Author Contributions: Conceptualization, A.A.d.N.P., C.P.d.S. and A.P.L.; Methodology, A.A.d.N.P., A.P.L.; Software, A.A.d.N.P., T.L.d.A.M.; Validation, A.A.d.N.P., C.P.d.S. and A.P.L.; Formal Analysis, A.A.d.N.P., R.S.S., C.P.d.S., T.L.d.A.M.; D.B.T.; Investigation, A.A.d.N.P. and C.P.d.S.; Resources, A.P.L. and D.B.T.; Data Curation, A.A.d.N.P.; Writing—Original Draft Preparation, A.A.d.N.P., R.S.S. and T.L.d.A.M.; Writing—Review and Editing, R.S.S., T.L.d.A.M., D.B.T., A.P.L.; Visualization, A.A.d.N.P., C.P.S., A.P.L.; Supervision, A.P.L.; Project Administration, A.P.L.; Funding Acquisition, A.P.L.

Funding: This research was funded by FAPESP (Fundação de Amparo à Pesquisa do Estado de São Paulo), grant numbers 2013/27064-9 and 2011/23895-8, and CAPES (Coordenação de Aperfeiçoamento de Pessoal de Nível Superior).

Acknowledgments: The authors would like to thank Cristiana Yoshida for the assistance during compression tests.

Conflicts of Interest: The authors declare no conflict of interest.

References

1. Montanheiro, T.L.A.; Montagna, L.S.; Patrulea, V.; Jordan, O.; Borchard, G.; Lobato, G.M.M.; Catalani, L.H.; Lemes, A.P. Evaluation of cellulose nanocrystal addition on morphology, compression modulus and cytotoxicity of poly (3-hydroxybutyrate-co-3-hydroxyvalerate) scaffolds. *J. Mater. Sci.* **2019**, *54*, 7198–7210. [[CrossRef](#)]
2. Armentano, I.; Dottori, M.; Fortunati, E.; Mattioli, S.; Kenny, J.M. Biodegradable polymer matrix nanocomposites for tissue engineering: A review. *Polym. Degrad. Stab.* **2010**, *95*, 2126–2146. [[CrossRef](#)]
3. Wang, Q.; Hou, R.; Cheng, Y.; Fu, J. Super-tough double-network hydrogels reinforced by covalently compositing with silica-nanoparticles. *Soft Matter* **2012**, *8*, 6048–6056. [[CrossRef](#)]
4. Kufelt, O.; El-Tamer, A.; Sehring, C.; Meißner, M.; Schlie-Wolter, S.; Chichkov, B.N. Water-soluble photopolymerizable chitosan hydrogels for biofabrication via two-photon polymerization. *Acta Biomater.* **2015**, *18*, 186–195. [[CrossRef](#)] [[PubMed](#)]
5. De Mesquita, J.P.; Donnici, C.L.; Teixeira, I.F.; Pereira, F.V. Bio-based nanocomposites obtained through covalent linkage between chitosan and cellulose nanocrystals. *Carbohydr. Polym.* **2012**, *90*, 210–217. [[CrossRef](#)]
6. Vimala, K.; Mohan, Y.M.; Sivudu, K.S.; Varaprasad, K.; Ravindra, S.; Reddy, N.N.; Padma, Y.; Sreedhar, B.; MohanaRaju, K. Fabrication of porous chitosan films impregnated with silver nanoparticles: A facile approach for superior antibacterial application. *Colloids Surf. B* **2010**, *76*, 248–258. [[CrossRef](#)] [[PubMed](#)]
7. Christensen, L.H.; Camitz, L.; Illigen, K.E.; Hansen, M.; Sarvaa, R.; Conaghan, P.G. The effects of polyacrylamide hydrogel in normal and osteoarthritic animal joints. *Osteoarthr. Cartilage* **2016**, *24*, S449–S450. [[CrossRef](#)]
8. Ferreira, S.D.O.; Montanheiro, T.L.A.; Ontagna, L.S.; Lemes, A.P. Study of cellulose nanocrystals and zinc nitrate hexahydrate addition in chitosan. *Mater. Res.* **2019**, *22*, 1–10. [[CrossRef](#)]
9. Ke, Y.; Wu, G.; Wang, Y. PHBV/PAM scaffolds with local oriented structure through UV polymerization for tissue engineering. *Biomed Res. Int.* **2014**, *2014*, 157987. [[CrossRef](#)]
10. Hong, Y.; Song, H.; Gong, Y.; Mao, Z.; Gao, C.; Shen, J. Covalently crosslinked chitosan hydrogel: Properties of in vitro degradation and chondrocyte encapsulation. *Acta Biomater.* **2007**, *3*, 23–31. [[CrossRef](#)]
11. Liu, Y.; Chen, W.; Kim, H. pH-responsive release behavior of genipin-crosslinked chitosan/poly(ethylene glycol) hydrogels. *J. Appl. Polym. Sci.* **2012**, *125*, 36899. [[CrossRef](#)]

12. Gaharwar, A.K.; Peppas, N.A.; Khademhosseini, A. Nanocomposite hydrogels for biomedical applications. *Biotechnol. Bioeng.* **2014**, *111*, 441–453. [[CrossRef](#)]
13. Khoushab, F.; Yamabhai, M. Chitin research revisited. *Mar. Drugs* **2010**, *8*, 1988–2012. [[CrossRef](#)]
14. Gonsalves, A.A.; Araújo, C.R.M.; Soares, N.A.; Goulart, M.O.F.; Abreu, F.C. de Diferentes estratégias para a reticulação de quitosana. *Quim. Nova* **2011**, *34*, 1215–1223. [[CrossRef](#)]
15. Hortigüela, M.J.; Aranaz, I.; Gutiérrez, M.C.; Ferrer, M.L.; Del Monte, F. Chitosan gelation induced by the in situ formation of gold nanoparticles and its processing into macroporous scaffolds. *Biomacromolecules* **2011**, *12*, 179–186. [[CrossRef](#)]
16. Montanheiro, T.L.A.; Montagna, L.S.; de Farias, M.A.; Lemes, A.P. Cytotoxicity and physico-chemical evaluation of acetylated and pegylated cellulose nanocrystals. *J. Nanopart. Res.* **2018**, *20*. [[CrossRef](#)]
17. Li, Q.; Zhou, J.; Zhang, L. Structure and properties of the nanocomposite films of chitosan reinforced with cellulose whiskers. *J. Polym. Sci. Part B Polym. Phys.* **2003**, *47*, 1069–1077. [[CrossRef](#)]
18. Geng, C.Z.; Hu, X.; Yang, G.; Zhang, Q.; Chen, F.; Fu, Q. Mechanically reinforced chitosan/cellulose nanocrystals composites with good transparency and biocompatibility. *Chinese J. Polym. Sci.* **2015**, *33*, 61–69. [[CrossRef](#)]
19. El Miri, N.; Abdelouahdi, K.; Zahouily, M.; Fihri, A.; Barakat, A.; Solhy, A.; El Achaby, M. Bio-nanocomposite films based on cellulose nanocrystals filled polyvinyl alcohol/chitosan polymer blend. *J. Appl. Polym. Sci.* **2015**, *132*, 1–13. [[CrossRef](#)]
20. Pereda, M.; Dufresne, A.; Aranguren, M.I.; Marcovich, N.E. Polyelectrolyte films based on chitosan/olive oil and reinforced with cellulose nanocrystals. *Carbohydr. Polym.* **2014**, *101*, 1018–1026. [[CrossRef](#)]
21. Khan, A.; Khan, R.A.; Salmieri, S.; Tien, C.L.; Riedl, B.; Bouchard, J.; Chauve, G.; Tan, V.; Kamal, M.R.; Lacroix, M. Mechanical and barrier properties of nanocrystalline cellulose reinforced chitosan based nanocomposite films. *Carbohydr. Polym.* **2012**, *90*, 1601–1608. [[CrossRef](#)]
22. Algan, C. Electrospinning of Chitosan-Based Nanocomposites Reinforced with Biobased Nanocrystals for Biomedical Applications. Master's Thesis, Luleå University of Technology, Lulea, Sweden, October 2013.
23. Sultana, N.; Wang, M. PHBV tissue engineering scaffolds fabricated via emulsion freezing / freeze-drying: effects of processing parameters. *Int. Conf. Biomed. Eng. Technol.* **2011**, *11*, 29–34.
24. Sankar, D.; Chennazhi, K.P.; Nair, S.V.; Jayakumar, R. Fabrication of chitin/poly(3-hydroxybutyrate-co-3-hydroxyvalerate) hydrogel scaffold. *Carbohydr. Polym.* **2012**, *90*, 725–729. [[CrossRef](#)]
25. Shaheen, T.I.; Emam, H.E. Sono-chemical synthesis of cellulose nanocrystals from wood sawdust using Acid hydrolysis. *Int. J. Biol. Macromol.* **2018**, *107*, 1599–1606. [[CrossRef](#)]
26. Song, K.; Ji, Y.; Wang, L.; Wei, Y.; Yu, Z. A green and environmental benign method to extract cellulose nanocrystal by ball mill assisted solid acid hydrolysis. *J. Clean. Prod.* **2018**, *196*, 1169–1175. [[CrossRef](#)]
27. Wang, Z.; Yao, Z.; Zhou, J.; He, M.; Jiang, Q.; Li, S.; Ma, Y. International journal of biological macromolecules isolation and characterization of cellulose nanocrystals from pueraria root residue. *Int. J. Biol. Macromol.* **2019**, *129*, 1081–1089. [[CrossRef](#)]
28. Mutjé, P.; Lòpez, A.; Vallejos, M.E.; Lòpez, J.; Vilaseca, F. Full exploitation of Cannabis sativa as reinforcement / filler of thermoplastic composite materials. *Composites Part A* **2007**, *38*, 369–377. [[CrossRef](#)]
29. Celebi, H.; Kurt, A. Effects of processing on the properties of chitosan/cellulose nanocrystal films. *Carbohydr. Polym.* **2015**, *133*, 284–293. [[CrossRef](#)]
30. Pujana, M.A.; Pérez-álvarez, L.; Carlos, L.; Iturbe, C.; Katime, I. Biodegradable chitosan nanogels crosslinked with genipin. *Carbohydr. Polym.* **2013**, *94*, 836–842. [[CrossRef](#)]
31. Butler, M.F.; Ng, Y.; Pudney, P.D.A. Mechanism and kinetics of the crosslinking reaction between biopolymers containing primary amine groups and genipin. *J. Polym. Sci. Part. A Polym. Chem.* **2003**, *41*, 3941–3953. [[CrossRef](#)]
32. Bi, L.; Cao, Z.; Hu, Y.; Song, Y.; Yu, L.; Yang, B.; Mu, J.; Huang, Z.; Han, Y. Effects of different cross-linking conditions on the properties of genipin-cross-linked chitosan/collagen scaffolds for cartilage tissue engineering. *J. Mater. Sci. Mater. Med.* **2011**, *22*, 51–62. [[CrossRef](#)]
33. Wang, S.; Sun, C.; Guan, S.; Li, W.; Xu, J.; Ge, D.; Zhuang, M.; Liu, T.; Ma, X. Chitosan/gelatin porous scaffolds assembled with conductive poly(3,4-ethylenedioxythiophene) nanoparticles for neural tissue engineering. *J. Mater. Chem. B* **2017**, *5*, 4774–4788. [[CrossRef](#)]

34. Yang, G.; Xiao, Z.; Long, H.; Ma, K.; Zhang, J.; Ren, X.; Zhang, J. Assessment of the characteristics and biocompatibility of gelatin sponge scaffolds prepared by various crosslinking methods. *Sci. Rep.* **2018**, *8*, 1616. [[CrossRef](#)]
35. Carvalho, I.C.; Mansur, H.S. Engineered 3D-scaffolds of photocrosslinked chitosan-gelatin hydrogel hybrids for chronic wound dressings and regeneration. *Mater. Sci. Eng. C* **2017**, *78*, 690–705. [[CrossRef](#)]
36. Naseri, N.; Poirier, J.M.; Girandon, L.; Fröhlich, M.; Oksman, K.; Mathew, A.P. 3-Dimensional porous nanocomposite scaffolds based on cellulose nanofibers for cartilage tissue engineering: Tailoring of porosity and mechanical performance. *RSC Adv.* **2016**, *6*, 5999–6007. [[CrossRef](#)]
37. Wu, T.; Farnood, R.; Kelly, K.O.; Chen, B. Mechanical behavior of transparent nano fibrillar cellulose–chitosan nanocomposite films in dry and wet conditions. *J. Mech. Behav. Biomed. Mater.* **2014**, *32*, 279–286. [[CrossRef](#)]
38. Ferreira, F.V.; Dufresne, A.; Pinheiro, I.F.; Souza, D.H.S.; Gouveia, R.F.; Mei, L.H.I.; Lona, L.M.F. How do cellulose nanocrystals affect the overall properties of biodegradable polymer nanocomposites: A comprehensive review. *Eur. Polym. J.* **2018**, *108*, 274–285. [[CrossRef](#)]
39. Zhu, H.; Shen, J.; Feng, X.; Zhang, H.; Guo, Y.; Chen, J. Fabrication and characterization of bioactive silk fibroin/wollastonite composite scaffolds. *Mater. Sci. Eng. C* **2010**, *30*, 132–140. [[CrossRef](#)]
40. Sabree, I.; Gough, J.E.; Derby, B. Mechanical properties of porous ceramic scaffolds: Influence of internal dimensions. *Ceram. Int.* **2015**, *41*, 8425–8432. [[CrossRef](#)]



© 2019 by the authors. Licensee MDPI, Basel, Switzerland. This article is an open access article distributed under the terms and conditions of the Creative Commons Attribution (CC BY) license (<http://creativecommons.org/licenses/by/4.0/>).